Crystalline Ceramic Waste Forms: Comparison of Reference Process for Ceramic Waste Form Fabrication

Fuel Cycle Research & Development

Prepared for
U.S. Department of Energy
Separations and Waste Forms

K.S. Brinkman, J. Amoroso and J.C. Marra
Savannah River National Laboratory
M. Tang
Los Alamos National Laboratory

August 13, 2013

FCRD-SWF-2013-000229
SRNL-STI-2013-00442

SUMMARY

The research conducted in this work package is aimed at taking advantage of the long term thermodynamic stability of crystalline ceramics to create more durable waste forms (as compared to high level waste glass) in order to reduce the reliance on engineered and natural barrier systems. Durable ceramic waste forms that incorporate a wide range of radionuclides have the potential to broaden the available disposal options and to lower the storage and disposal costs associated with advanced fuel cycles. Assemblages of several titanate phases have been successfully demonstrated to incorporate radioactive waste elements, and the multiphase nature of these materials allows them to accommodate variation in the waste composition. Recent work has shown that they can be produced from a melting and crystallization process. The objective of this report is to explore the phase formation and microstructural differences between lab scale melt processing in varying gas environments with alternative densification processes such as Hot Pressing (HP) and Spark Plasma Sintering (SPS).

The waste stream used as the basis for the development and testing is a simulant derived from a combination of the projected Cs/Sr separated stream, the Trivalent Actinide - Lanthanide Separation by Phosphorous reagent Extraction from Aqueous Komplexes (TALSPEAK) waste stream consisting of lanthanide fission products, the transition metal fission product waste stream resulting from the transuranic extraction (TRUEX) process, and a high molybdenum concentration with relatively low noble metal concentrations.

Melt processing as well as solid state sintering routes SPS and HP demonstrated the formation of the targeted phases; however differences in microstructure and elemental partitioning were observed. In SPS and HP samples, hollandite, pervoskite/pyrochlore, zirconolite, metallic alloy and TiO_2 and Al_2O_3 were observed distributed in a network of fine grains with small residual pores. The titanate phases that incorporate M^{+3} rare earth elements were observed to be distinct phases (ex. $Nd_2Ti_2O_7$) with less degree of substitution as compared to the more homogeneous melt processed samples where a high degree of substitution and variation of composition within grains was observed. Liquid phase sintering was enhanced in reducing gas environments and resulted in large (10-200 microns) irregular shaped grains along with large voids associated with the melt process; SPS and HP samples exhibited finer grain size with smaller voids. Metallic alloys were observed in the bulk of the sample for SPS and HP samples, but were found at the bottom of the crucible in melt processed trials. These results indicate that for a first melter trial, the targeted phases can be formed in air by utilizing Ti/TiO_2 additives which aid phase formation and improve the electrical conductivity. Ultimately, a melter run in reducing gas environments would be beneficial to study differences in phase formation and elemental partitioning.

CONTENTS

FIGURES

TABLES

ABBREVIATIONS

CCIM	Cold Crucible Induction Melter
DOE	Department of Energy
EDAX	Energy Dispersive Spectroscopy
FCR&D	Fuel Cycle Research and Development
HLW	High Level Waste
HP	Hot Pressing (uniaxial)
HIP	Hot Isostatic Pressing
PUREX	Plutonium, Uranium, Extraction Processes
RedOx	Reduction/Oxidation
REE	Rare Earth Element
SEM	Scanning Electron Microscopy
SRNL	Savannah River National Laboratory
SYNROC	Titanium based ceramic substance that can incorporate nuclear waste
TALSPEAK	Trivalent Actinide - Lanthanide Separation by Phosphorous reagent Extraction from Aqueous Komplexes
TRUEX	Transuranic Extraction
XANES	X-ray Absorption Near Edge Structure
XRD	X-ray Diffraction
XPS	X-ray Photoelectron Spectroscopy

ACKNOWLEDGEMENTS

The authors would like to thank Henry Ajo, David Best, David Missimer, Elise Fox, Phyllis Workman, Pat Simmons, Whitney Riley, Mark Jones, and Curtis Johnson of SRNL for their assistance with sample preparation and characterization. The Hot Pressing and Spark Plasma Sintering samples analyzed in this work were fabricated at Clemson University by Prof. Jian He under the subcontract "SCN0010 Alternative Sintering of Waste Forms."

This work was supported by the U.S. Department of Energy, Office of Nuclear Energy, under Contract DE-AC02-06CH11357.

1. INTRODUCTION

Efforts being conducted by the United States Department of Energy (DOE) under the Fuel Cycle Research and Development (FCR&D) program are aimed at making potential U.S. fuel cycle options more effective by the development of next generation waste management technologies.[1] One envisioned fuel reprocessing technology would separate the fuel into several fractions, thus, partitioning the waste into groups with common chemistry. Ceramic (or crystalline) waste forms incorporate the radionuclides in the waste as part of the crystal structure.[2] As such, ceramic forms are tailored to create certain minerals (i.e. unique crystalline structures) that will host the radionuclides by binding them in their specific crystalline network. Tailoring of a ceramic waste form is based on the knowledge that there are many naturally produced minerals containing radioactive and non-radioactive species very similar to the radionuclides of concern in wastes from fuel reprocessing. The research conducted in this work package is aimed at taking advantage of the long term thermodynamic stability of crystalline ceramics to create more durable waste forms (as compared to high level waste (HLW) glass) in order to reduce the reliance on engineered and natural barrier systems. Durable ceramic waste forms that incorporate a wide range of radionuclides have the potential to broaden the available disposal options and to lower the storage and disposal costs associated with advanced fuel cycles.

Titanate ceramics have been thoroughly studied for use in immobilizing nuclear wastes (e.g., the synthetic rock, or "SYNROC" family) due to their natural resistance to leaching in water.[2, 3] Assemblages of several titanate phases have been successfully demonstrated to incorporate radioactive waste elements, and the multiphase nature of these materials allows them to accommodate variation in the waste composition.[4] While these materials are typically densified via hot isostatic pressing (HIP), recent work has shown that they can also be produced from a melt. For example, demonstrations have been completed using the Cold Crucible Induction Melter (CCIM) technology to produce several crystalline ceramic waste forms, including murataite-rich ceramics,[5] zirconolite/pyrochlore ceramics,[6] Synroc-C (zirconolite, hollandite, perovskite),[7] aluminotitanate ceramics, and zirconia.[8] This production route is advantageous since melters are already in use for defense HLW vitrification in several countries, and melter technology greatly reduces the potential for airborne contamination as compared to powder handling operations associated with hot isostatic pressing.

Previous reports completed in FY12 summarized the reference ceramic compositions and the results of initial melt processing for several targeted waste streams of interest to the FCR&D program[9, 10]. In agreement with previous attempts at melt processing Mo containing SYNROC type ceramics in oxidizing environments, the Savannah River National Laboratory (SRNL) designed crystalline ceramics melted in air showed evidence of non-durable molybdate phase formation[11]. Several strategies to address this issue were suggested in the FY12 reports including i) tailoring the hollandite stoichiometry to make Cs incorporation more favorable, ii) the addition of solid state reducing agents such as Ti metal to the batch, and iii) melt processing in reducing gas environments (1%H_2 balance Argon). The current report on FY13 work summarizes the results of these experiments aimed at varying the composition and reducing conditions in lab scale melts. In addition, this report presents an initial comparison of various reference processes for waste form fabrication including melt processing, hot pressing and spark plasma sintering with a focus on phase formation, microstructure and elemental partitioning. A premise of this work is that if the targeted crystalline phases are formed, the resulting durability will be comparable to SYNROC performance in the literature. Durability and leaching studies are not addressed in this report.

2. SINGLE PHASE HOLLANDITE

Cs is one of the more problematic fission product radionuclides to immobilize due to its high volatility at elevated temperatures, ability to form water soluble compounds, and its mobility in many host materials. A hollandite-type crystal structures appears to be a good candidates for Cs immobilization compared to other proposed silicate or phosphate ceramics which are difficult to fabricate as single phase wasteforms with high densities, or to nuclear glasses in which the alkaline elements are the most mobile waste species in aqueous environments. There are natural analogues of hollandite including ankagite, found in dolomitic marble in the Apuan Alps in Tuscany, Italy.[12] There has been limited work on the melt processing of single phase hollandite materials. Existing literature has focused Cs-rich waste targeted in dual phase hollandite/rutile mixtures fabricated via melt processing in air.[13] Hollandite formation based on dopants of Zn, Co, or Ni were successfully demonstrated in binary systems by melt processing in air. However, it is believed that reducing environments will be required to avoid molybdate (Cs-Mo) phase formation in the multiphase FCR&D waste forms of interest. This work has focused on tailoring the compositions and conditions that enable Cs incorporation into the hollandite phase under reducing conditions. The following section describes the choice of composition and processing conditions for the hollandite phase.

2.1. Composition and Processing Conditions

Although it is difficult to form a $(Ba_xCs_y)(Ti,Al)^{+3}{}_{2x+y}(Ti^{+4}{}_{8-2x-y})O_{16}$ single phase hollandite in oxidizing atmospheres, other M^{+3} elements such as Fe^{3+} can be substituted into the $(Ba_xCs_y)(Ti,Al)^{+3}{}_{2x+y}(Ti^{+4}{}_{8-2x-y})O_{16}$ phase targeting $Ba_{1.0}Cs_{0.28}Al_{1.46}Fe_{0.82}Ti_{5.72}O_{16}$ which has been shown to form a stable single phase compound. Recently, single phase hollandite materials containing mixtures of divalent and trivalent cations have been fabricated by solution mixtures and oxide routes based on the general formula $(Ba_xCs_y)(M^{+3}{}_zTi^{+4}{}_{8-z})O_{16}$ with M=Mn^{+3}, Fe^{+3}, Ga^{+3}, Cr^{+3}, Sc^{+3}, Ti^{+3}, Ni^{+2}, Co^{+2}, Zn^{+2}, and Mg^{+2} where z = 2x+y for trivalent cations and z = x+y/2 for divalent cations for charge compensation.[14-17] In general, many of those trivalent and divalent cations were effective in promoting Cs incorporation into the hollandite, but also promoted secondary phase formation. Dopants which have the atomic radius appropriate for the M^{+3} site in the hollandite are not found in the anticipated waste streams. However, taking into consideration the corrosion products and other additives from the separations processes results in appreciable concentrations of Cr_2O_3 and/or Fe_2O_3 (~1-10 wt%) arising from Purex or JW-A processing contamination[18, 19]. The presence of Fe^{+3} (coexisting with Al^{+3}) in the B site of the structure facilitated Cs incorporation via calcining at 1000°C and air sintering at 1200°C. In addition, iron oxide and chromium oxide additions may improve the densification and melting properties due to the lower melting point as compared to Al_2O_3 rich compositions.

Cr was identified as a potential additive because it has consistently resulted in single phase hollandite formation in air throughout the literature. There is very little data published concerning the melt processing or fabrication of the Cr analogue in varying redox conditions. The Al-Fe containing hollandite has been widely studied, however this work developed a new Cr-Al-Fe composition to exploit the Cr ionic radius (less than Fe^{+3} but greater than Al^{+3}) which is expected to promote single phase formation while maximizing Cs incorporation. A pure Fe analogue, expected to be multiphase and exhibit poor durability, was included as a baseline for the comparison of results. The three compositions studied in this work were: $Ba_{1.0}Cs_{0.3}Fe_{2.3}Ti_{5.7}O_{16}$ – referred to as Fe-Hol, $Ba_{1.0}Cs_{0.3}Cr_{2.3}Ti_{5.7}O_{16}$ – referred to as Cr-Hol, and $Ba_{1.0}Cs_{0.3}Cr_{1.0}Al_{0.3}Fe_{1.0}Ti_{5.7}O_{16}$ – referred to as Cr/Al/Fe-Hol.

The batch preparation of the three compositions was as follows: stoichiometric amounts of reagent-grade oxide and carbonate powders were mixed to make 100g of each hollandite material. These powders were

combined in a 500ml plastic bottle with zirconia milling media, filled 2/3 full with deionized water, and agitated in a tumbler mixer for 1 hour. The resulting slurry was poured into a separate pan along with additional rinse water used to collect any batch material remaining on the milling media and bottles. Each pan was transferred to an oven where the slurry was dried for several days at 90°C. The dried material was bagged and used as feed stock for synthesis experiments. In addition to compositional variants, all samples were processed with excess Ti metal and TiO_2 (referred to in this text as Ti/TiO_2 buffer). The Ti metal was added – <230 mesh, ~2.0 wt. % – to control the RedOx state during processing and in effect, phase formation. TiO_2 was added – ~6.5 wt. % – to buffer the reducing effects of the Ti metal on TiO_2.[10] In this fashion, a combination of gas phase environment and solid state reducing agents were used to vary the RedOx conditions using different processing techniques: i) melt processing of compositions with and without Ti/TiO_2 buffer in air and 1%H_2 /balance Argon gas environments, ii) spark plasma sintering with a Ti/TiO_2 buffer in N_2 gas at varying temperatures and iii) hot press with and without Ti/TiO_2 buffer in N_2 gas at varying temperatures.

The microstructures of select samples are presented along with a table indicating the elemental composition and crystalline phases observed in each section. A summary of the entirety of results on single phase hollandite across composition and processing method and reducing conditions is summarized in a table at the end of Section 2.4.

2.2. Melt Processing

Approximately 20g samples of feed stock were loosely placed into a covered alumina crucible. The samples were heated in air and in 1% H_2 (balance Argon) reducing atmosphere. Samples were heated at approximately 15^{o}C/min, held at 1500°C for 20 minutes, and furnace cooled (powered off furnace). The resulting material was subsequently characterized. FY12 work that focused on melt processing in air demonstrated Cr or a combination of Cr and Al in the target hollandite composition, along with Ti/TiO_2 buffers, resulted in single phase hollandite formation with the requisite Cs-incorporation[10]. The current work is focused on evaluating Cr-Hol and Cr/Al/Fe-Hol phase formation in reducing conditions which are anticipated to be utilized in multiphase wasteforms. The following sections show the microstructure and phase identification of three hollandite compositions *without* Ti/TiO_2 buffer melt processed in 1%H_2 balance Argon reducing gas conditions.

2.2.1. Fe-Hollandite

Figure 2-1 displays the microstructure and Table 2-1 summarizes the phase formation of a Fe-Hollandite fabricated by melt and crystallization process in 1%H_2 balance Argon *without* Ti/TiO_2 buffer. The microstructure was crystalline with some porosity and voids as would be expected from a melt process. The Fe-Hollandite sample showed the presence of several secondary phases including spinels, titanates and aluminates along with the primary hollandite phase. In particular, Cs was found in the $CsAlTiO_4$ phase which is known to be less durable than hollandite which could adversely affect Cs retention during aqueous corrosion.

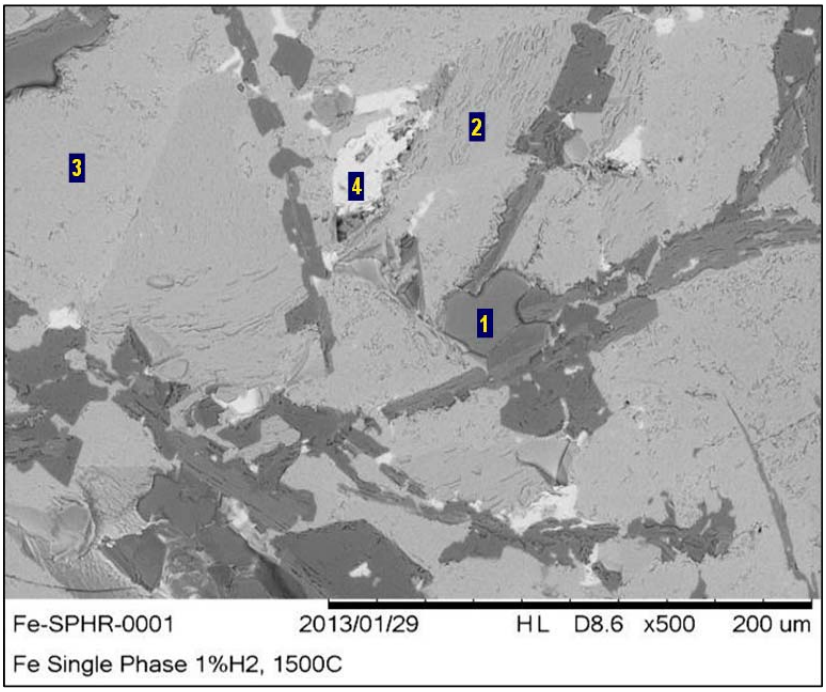

Figure 2-1. Fe-Hollandite Fabricated by Melting and Crystallizing in 1%H_2 balance Argon *without* Ti/TiO_2 buffer Backscattered Electron Micrograph

Table 2-1. Fe-Hollandite Fabricated by Melting and Crystallizing in 1%H_2 *without* Ti/TiO_2 buffer Fabricated by Melting and Crystallizing -Summary of Elements and Crystalline Phases
(*Crystalline phases determined from X-ray Diffraction XRD measurements and Energy Dispersive X-ray Spectroscopy EDAX elemental analysis)

Spot	Elements (Major, Minor)	Crystalline Phases*
1	O,Al,Fe,Ti	$FeAl_2O_4$, $(A^{+3})_2TiO_5$
2,3	O,Ti,Al,Fe,Ba, (Cs)	Hollandite
4	O, Ti, Cs, Al	$Cs_2Ti_2O_5$, $CsAlTiO_4$

2.2.2.Cr Hollandite

Figure 2-2 displays the phase microstructure and Table 2-2 summarizes the phase formation of Cr-Hollandite fabricated by a melt and crystallization process in 1%H_2 balance Argon *without* a Ti/TiO_2 buffer. The microstructure is indicative of a solid state reaction mechanism with limited evidence of melting. However, it is suspected that when incorporated into a multiphase waste form, the additional constituents comprising the melt will aid melt processing, even of the high refractory Cr-Hollandite composition. Single phase hollandite with Cs incorporation was primarily observed along with residual TiO_2.

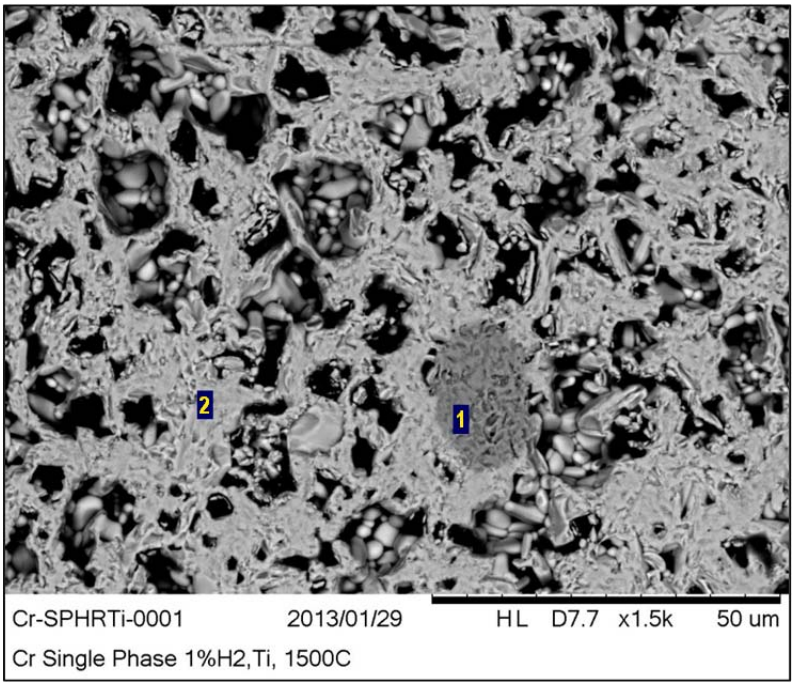

Figure 2-2. Cr-Hollandite Fabricated by Melting and Crystallizing in 1%H_2 balance Argon *without* Ti/TiO_2 buffer Backscattered Electron Micrograph

Table 2-2. Cr-Hollandite Fabricated by Melting and Crystallizing in 1%H_2 *without* Ti/TiO_2 buffer Fabricated by Melting and Crystallizing -Summary of Elements and Crystalline Phases
(*Crystalline phases determined from XRD measurements and EDAX elemental analysis)

Spot	Elements (Major, Minor)	Crystalline Phases*
1	O, Ti	TiO_2
2	O, Ti, Cr, Cs, Ba	Hollandite

2.2.3. Cr/Al/Fe Hollandite

Figure 2-3 displays the microstructure and Table 2-3 tabulates the phase formation of Cr/Al/Fe-Hollandite melt processed at 1500°C *without* Ti/TiO_2 buffer in 1%H_2 balance Argon reducing atmosphere. The observed microstructure is a combination of the Fe and Cr analogues; some areas of the sample appear to have completely melted (Fe) while others exhibit features of solid state sintering (Cr). The primary crystalline phase observed was hollandite along with Fe_2TiO_5 spinel secondary phases.

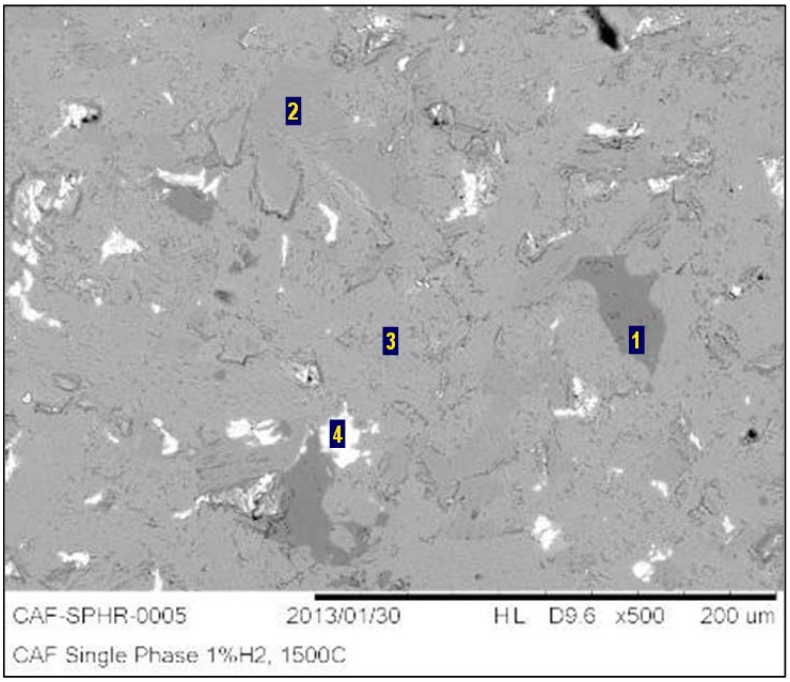

Figure 2-3. Cr/Al/Fe-Hollandite Fabricated by Melting and Crystallizing in 1%H_2 balance Argon *without* Ti/TiO_2 buffer Backscattered Electron Micrograph

Table 2-3. Cr/Al/Fe-Hollandite Fabricated by Melting and Crystallizing in 1%H_2 *without* Ti/TiO_2 buffer Fabricated by Melting and Crystallizing -Summary of Elements and Crystalline Phases *(*Crystalline phases determined from XRD measurements and EDAX elemental analysis)*

Spot	Elements (Major, Minor)	Crystalline Phases*
1	O,Fe,Al,Ti	$FeAl_2O_4$
2,3	O,Ti,Ba,Al,Cr,Fe	Hollandite
4	O,Ti,Cs,Al	$Cs_2Ti_2O_5$, $CsAlTiO_4$

2.3. Spark Plasma Sintering (SPS)

Spark Plasma Sintering (SPS) was conducted on a Dr. Sinter Model SPS 515S from Metals Processing Inc. Approximately 1g of powder batch was mixed *with* a Ti/TiO_2 buffer and loaded in a graphite die for SPS processing at temperatures between 1040 and 1240^{o}C.

2.3.1. Cr Hollandite

Figure 2-4 displays the microstructure and Table 2-5 tabulates the phase information for the Cr-Hollandite fabricated by SPS *with* Ti/TiO_2 buffer at 1240^{o}C. In general the SPS microstructure was relatively dense without the presence of large voids. Cs was observed in the primary hollandite phase, but was also observed in secondary $Cs_2Ti_2O_5$ phases.

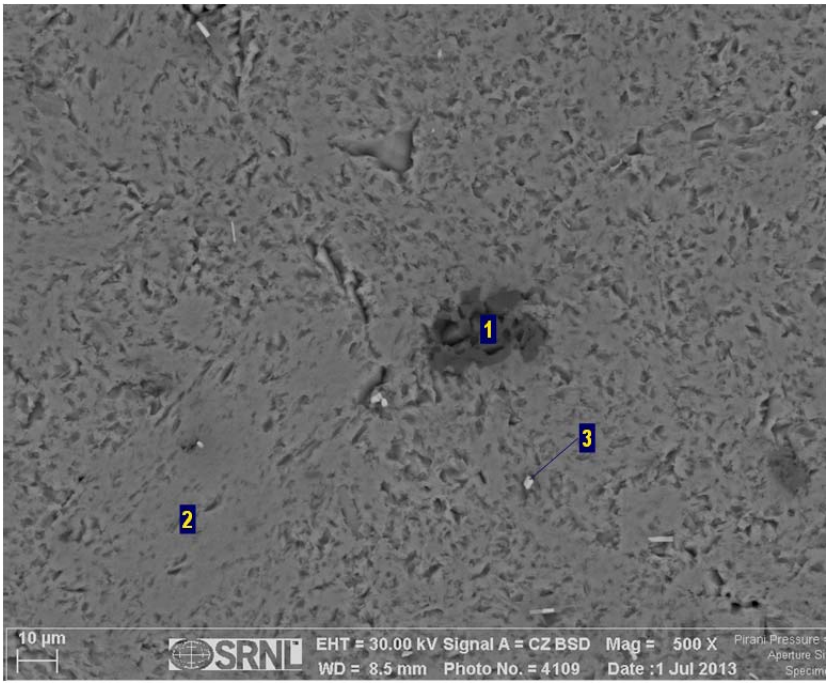

Figure 2-4. Cr-Hollandite Fabricated by SPS *with* Ti/TiO_2 buffer at 1240°C Backscattered Electron Micrograph

Table 2-4. Cr-Hollandite Fabricated by SPS *with* Ti/TiO_2 at 1240°C -Summary of Elements and Crystalline Phases *(*Crystalline phases determined from XRD measurements and EDAX elemental analysis)*

Spot	Elements (Major, Minor)	Crystalline Phases*
1	O, Ti	TiO_2
2	O, Ti, Cr, Ba, Cs	Hollandite
3	O, Ti, Cs	$Cs_2Ti_2O_5$, $FeAl_2O_4$

2.3.2. Cr/Al/Fe Hollandite

Figure 2-5 displays the microstructure and Table 2-5 tabulates the phases observed in Cr/Al/Fe-Hollandite *with* Ti/TiO_2 buffer fabricated by SPS at 1230°C. Small pores resulting from solid state sintering (~ 1 micron) were observed which were distributed throughout the microstructure. In addition to the primary Cs containing hollandite phase, there were $Cs_2Ti_2O_5$ and $(A^{+3})_2TiO_5$ with A^{+3}=Fe, Al, Cr secondary phases observed.

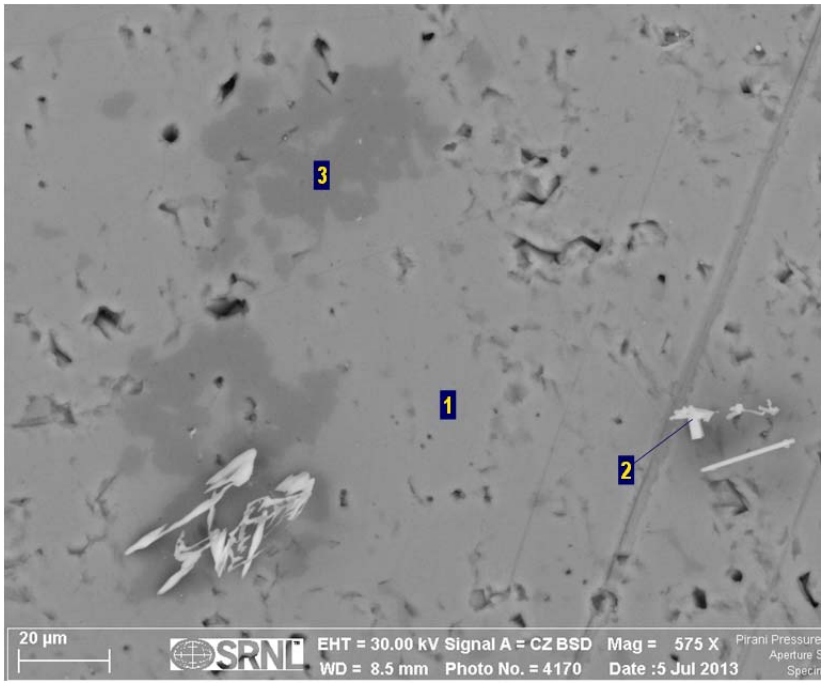

Figure 2-5. Cr/Al/Fe-Hollandite Fabricated by SPS *with* Ti/TiO_2 buffer at 1230°C Backscattered Electron Micrograph

Table 2-5. Cr/Al/Fe-Hollandite Fabricated by SPS *with* Ti/TiO_2 buffer at 1230°C -Summary of Elements and Crystalline Phases *(*Crystalline phases determined from XRD measurements and EDAX elemental analysis)*

Spot	Elements (Major, Minor)	Crystalline Phases*
1	O, Ti, Cr, Al, Fe, Ba, Cs	Hollandite
2	O, Ti, Cs	$Cs_2Ti_2O_5$
3	O, Ti, Cr, Al, Fe	$(A^{+3})_2TiO_5$

2.4. Hot Pressing (HP)

The hot pressing procedure consisted of an initial 10°C/min ramp to a temperature of 1200°C where the sample was held for 2 hours followed by a decrease of the temperature to 1000°C in 15 minutes and finally shutting off the furnace and allowing the sample to cool to room temperature in approximately 2.5 hours. The pressure was maintained at 40+/-1 MPa with nitrogen gas supplied at a flow rate of 40 ml/min during the hot press procedure.

2.4.1.Cr Hollandite

Figure 2-6 displays the microstructure and Table 2-6 tabulates the phases observed in Cr-Hollandite *with* Ti/TiO_2 buffer fabricated by HP at 1200°C for 2 hours (40MPA, N_2 gas). The sample appears relatively dense with small pores (~ 1-5 micron) which were distributed throughout the microstructure. In addition to the primary Cs containing hollandite phase, there was residual Cr_2O_3 and TiO_2 detected.

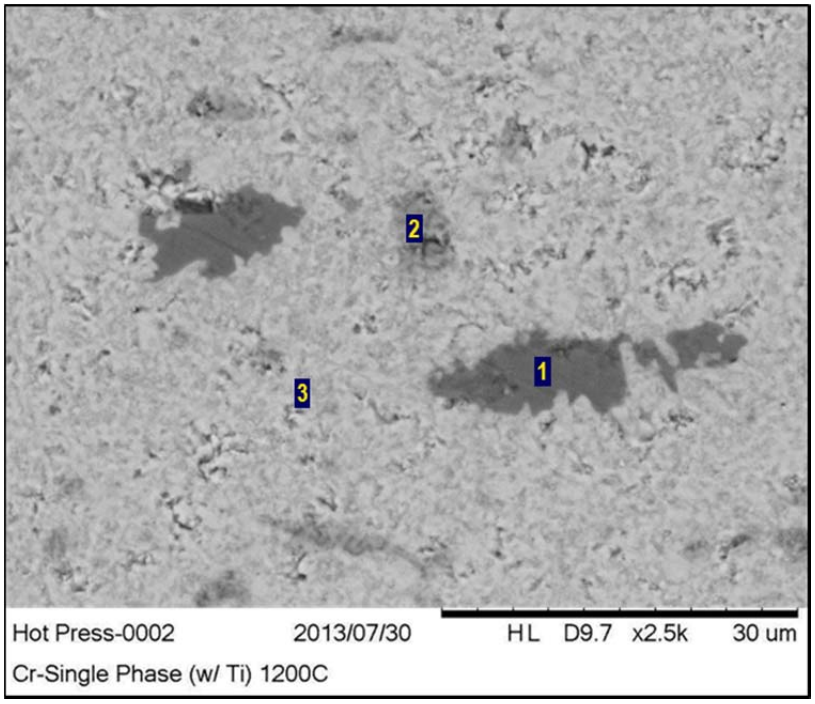

Figure 2-6. Cr-Hollandite *with* Ti/TiO_2 buffer Fabricated by HP at 40MPa under N_2 gas at 1200°C for 2 hours- Backscattered Electron Micrograph

Table 2-6. Cr -Hollandite *with* Ti/TiO_2 buffer Fabricated by HP at 40MPa under N_2 gas at 1200°C for 2 hours -Summary of Elements and Crystalline Phases *(*Crystalline phases determined from XRD measurements and EDAX elemental analysis)*

Spot	Elements (Major, Minor)	Crystalline Phases*
1	O,Ti	TiO_2
2	O,Cr	Cr_2O_3
3	O,Ti,Cr,Ba,Cs	Hollandite

2.4.2.Cr/Al/Fe Hollandite

Figure 2-7 displays the microstructure and Table 2-7 tabulates the phases observed in Cr/Al/Fe-Hollandite *with* Ti/TiO_2 buffer fabricated by HP at 1200°C for 2 hours (40MPA, N_2 gas). The sample appears is similar to the pure Cr analogue and is relatively dense with small pores (~ 1-5 micron) which were distributed throughout the microstructure. In addition to the primary Cs containing hollandite phase, there was residual Cr_2O_3 and Fe oxide and Al_2O_3 detected.

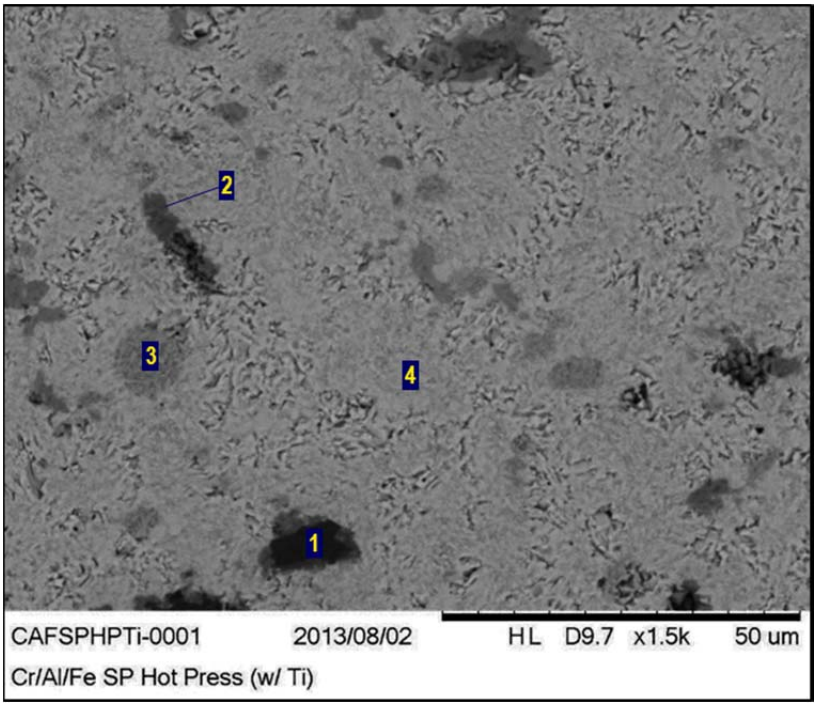

Figure 2-7. Cr/Al/Fe-Hollandite *with* Ti/TiO_2 buffer Fabricated by HP at 40MPa under N_2 gas at 1200°C for 2 hours- Backscattered Electron Micrograph

Table 2-7. Cr/Al/Fe-Hollandite *with* Ti/TiO_2 buffer Fabricated HP at 40MPa under N_2 gas at 1200°C for 2 hours -Summary of Elements and Crystalline Phases *(*Crystalline phases determined from XRD measurements and EDAX elemental analysis)*

Spot	Elements (Major, Minor)	Crystalline Phases*
1	O,Al	Al_2O_3
2	O,Fe, (Al)	Iron Oxide
3	O,Cr, (Fe)	Cr_2O_3
4	O,Ti,Cr,Ba,Cs	Hollandite

Table 2-8. Single Phase Hollandite Characterization Summary[a]

Short Identifier[a]	Major Phase	Minor Phase(s)[b]	Processing Conditions
Melt Processing			
Fe-SPH	Hollandite	Fe_2TiO_5; $Fe_2Ti_3O_9$	Air
Fe-SPH-Ti	Hollandite	$Fe_3Ti_3O_{10}$; $CsTiAlO_4$; Fe_2O_3	Air w/Ti-TiO_2
Fe-SPHR	Hollandite	Al_2TiO_5; $BaFe_{12}O_{19}$; $FeAl_2O_4$	1% H_2
Fe-SPHR-Ti	Hollandite	Al_2O_3; $FeAl_2O_4$	1% H_2 w/Ti-TiO_2
Cr-SPH	Hollandite		Air
Cr-SPH-Ti	Hollandite	TiO_2	Air w/Ti-TiO_2
Cr-SPHR	Hollandite		1% H_2
Cr-SPHR-Ti	Hollandite	TiO_2	1% H_2 w/Ti-TiO_2
CAF-SPH	Hollandite		Air
CAF-SPH-Ti	Hollandite	Fe_2TiO_4	Air w/Ti-TiO_2
CAF-SPHR	Hollandite	$FeAl_2O_4$	1% H_2
CAF-SPHR-Ti	Hollandite	$FeAl_2O_4$	1% H_2 w/Ti-TiO_2
Spark Plasma Sintering (SPS)			
Cr-SPH-SPS-1040	Hollandite	Cr_2O_3, $Cs_2Ti_2O_5$	1040°C w/Ti-TiO_2
Cr-SPH-SPS-1240	Hollandite	Cr_2O_3, $Cs_2Ti_2O_5$	1240°C w/Ti-TiO_2
CAF-SPH-SPS-1040	Hollandite		1040°C w/Ti-TiO_2
CAF-SPH-SPS-1230	Hollandite	Fe_2TiO_5	1230°C w/Ti-TiO_2
Hot Pressing			
Cr-SPH-HP	Hollandite	Cr_2O_3	N_2,1200°C
Cr-SPH-HP-Ti	Hollandite	Cr_2O_3	N_2,1200°C, w/Ti-TiO_2
CAF-SPH-HP	Hollandite	$BaFe_{12}O_{19}$	N_2,1200°C
CAF-SPH-HP-Ti	Hollandite		N_2,1200°C, w/Ti-TiO_2

Table 2-8 summarizes the phase formation versus composition and processing conditions for single phase hollandite samples fabricated in this study. Experiments have shown that reducing agents and atmospheres affect hollandite formation and Cs incorporation. Under reducing conditions, samples batched with Fe_2O_3 are expected to be rich in FeO and Al_2O_3 leading to $FeAl_2O_4$ spinel formation. Thus, the hollandite composition (relative to targeted hollandite) was deficient in Fe and Al. The Fe-Al compounds were observed in all Fe containing samples irrespective of processing method, whereas the Cr-hollandite samples exhibited single phase hollandite formation under both reducing and oxidizing environments. X-ray PhotoElectron Spectroscopy (XPS) and X-ray Absorption spectroscopy (XANES) were used to probe the Cr and Fe oxidization states in melt processed samples. The results indicated that the Cr valence was unchanged across the reducing spectrum from air to 1%H_2 gas *with* Ti/TiO_2 buffer additions, while the Fe was reduced under reducing conditions.[20] The use of Cr and Ti/TiO_2 buffer appears to stabilize the hollandite structure and promote Cs incorporation. This work suggests that Cr preferentially enters the hollandite phase (even in the presence of competing phases) because it does not

[a] "Fe-…" targeted $Ba_{1.0}Cs_{0.3}\mathbf{Fe}_{2.3}Ti_{5.7}O_{16}$ Hollandite; "Cr-…" targeted $Ba_{1.0}Cs_{0.3}\mathbf{Cr}_{2.3}Ti_{5.7}O_{16}$ Hollandite; "CAF-…" targeted $Ba_{1.0}Cs_{0.3}\mathbf{Cr}_{1.0}\mathbf{Al}_{0.3}\mathbf{Fe}_{1.0}Ti_{5.7}O_{16}$ Hollandite.

[b] The phases listed in this column have a known amount of ambiguity as they are based on semi-quantitative analysis and previous conclusions; they should be taken to represent the general types of compounds forming and species in those compounds.

readily form compounds with Cs and it is not easily susceptible to reduction. The potential drawback to Cr additions includes the elevated temperatures required for melting as compared to Fe/Al analogues.

This work demonstrated the melt processing of single phase hollandite in air and reducing environments by tailoring the composition and using solid state Ti/TiO_2 buffer. The hollandite phase formation incorporating Cs is comparable with the HP and SPS methods investigated. Major differences between the melt processed and alternative sintering routes include an increase in grain size in melt processed samples accompanied by few, but large voids (> 10 micron size) due to the melt process. In contrast, the SPS and HP process have many, but small voids (~ 1-5 micron in size) well distributed throughout the materials. With the observed differences in microstructure with varying process conditions, the impact of microstructure on materials durability should be the focus of future studies. These results indicate that Cs-incorporation into a stable hollandite phase is possible under the reducing conditions anticipated in multi-phase systems. However, while reducing conditions may eliminate the formation of non-durable molybdate phases, these same reducing conditions increase the tendency for variable valance species such as Fe to form secondary phases along with the targeted hollandite. The ability to tailor hollandite stoichiometry in complex multiphase systems may be a key factor in choice of processing routes and ultimately material performance.

3. MULTIPHASE SYTEMS

The single phase hollandite compositions Cr-Hol, and Cr/Al/F-Hol which demonstrated the best phase formation under reducing conditions were incorporated into multiphase ceramics targeting hollandite, perovskite/pyrochlore and zirconolite phase assemblages from combined Cs/Sr, lanthanide, and transition metal (including Mo) waste streams.

3.1. Composition Development and Processing Conditions

The design and calculation of reference ceramic host systems for FCR&D waste streams was presented in the FY12 report “Crystalline Ceramic Waste Forms: Reference Formulation Report”.[9] In this work, optimized single phase hollandite compositions based on Cr and Cr/Al/Fe additions were incorporated into multiphase ceramics targeting hollandite, perovskite/pyrochlore and zirconolite phase assemblages from combined Cs/Sr, lanthanide, and transition metal (including Mo) waste streams. Two different multiphase compositions were prepared as described in Table 3-1 with ~25 weight % waste loading and varying concentrations of CaO, Al_2O_3, BaO, Cr_2O_3, Fe_2O_3 and TiO_2 additives. The chemical composition (batch sheets) of these two samples compared to literature SYNROC-C formulations is given in Table 3-2. Details of the simulated waste, additives, and melting and crystalizing processes, and characterization are described in the FY10 and FY11 and FY12 reports.[9, 21, 22]

Similar to the single phase hollandite work presented in Section 2, a combination of gas phase environment and solid state reducing agents were used to vary the redox conditions using different processing techniques: i) melt processing of compositions *with* and *without* Ti/TiO_2 buffer in air and $1\%H_2$ /balance Argon gas environments, ii) vacuum induction melting at 10^{-6} atm and 1500^oC *with* and *without* Ti/TiO_2 buffer iii) spark plasma sintering *with* a Ti/TiO_2 buffer in N_2 gas at varying temperatures and iv) hot press *with* and *without* Ti/TiO_2 buffer in N_2 gas at varying temperatures.

The microstructures of select samples are presented along with a table indicating the elemental composition and crystalline phases observed in each section. A summary of the entirety of results on multiphase waste forms across composition and processing method and reducing conditions is summarized in a table at the end of Section 3.5.

Table 3-1. Ceramic Waste Form Compositions for SRNL Multiphase Melt Samples compared to SYNROC-C[11]; weight percent of oxide component

Composition	Cr-MP	CAF-MP	SYNROC-C[a]
Waste	24.58	24.66	19.81
Al_2O_3	0	1.27	4.63
TiO_2	49.01	49.16	61.4
CaO	1.38	1.39	9.59
BaO	10.52	10.56	4.57
Fe_2O_3	0	6.65	0.894
Cr_2O_3	14.50	6.33	-

Table 3-2. Chemical Composition (Batch Sheets) of SRNL Multiphase Melt Samples compared to SYNROC-C[11]; weight percent of oxide component

Oxides	Cr-MP	CAF-MP	SYNROC-C[a]
Al_2O_3	0.00	1.27	6.77
CaO	1.38	1.39	10.42
CdO	0.11	0.11	-
Cr_2O_3	14.50	6.33	-
Eu_2O_3	0.17	0.17	0.894
Fe_2O_3	0.00	6.65	1.15
Gd_2O_3	0.16	0.16	x
SrO	0.98	0.98	1.17
TiO_2	49.01	49.16	58.3
ZrO_2	2.98	2.99	8.4
BaO	12.72	12.76	4.73
Ce_2O_3	3.09	3.10	x
Cs_2O	2.87	2.88	0.53
La_2O_3	1.58	1.58	x
MoO_3	0.84	0.85	2.36
Nd_2O_3	5.22	5.23	x
Pr_2O_3	1.44	1.45	x
SeO_2	0.08	0.08	-
SnO_2	0.07	0.07	-
Sm_2O_3	1.07	1.08	x
TeO_2	0.65	0.66	-
Y_2O_3	0.63	0.63	x
Rb_2O	0.42	0.42	-
Total REE_2O_3	13.19	13.23	6.10[b]

[a] SYNCROC-C cited was material prepared by melting of an oxide-nitrate mixture. Crystalline oxides of Ca,Ba,Fe,Ni,Al,Mo,Ti and Zr and nitrates of Cs,Sr,Nd,Gd and Ce were mixed and melt processed. SYNROC-C samples also contained oxide additions of Si, Mg, Co, Ni, Na, and K.[11] 11. Sobolev, I.A., et al., *Comparative Study of Synroc-C Ceramics Produced by Hot-Pressing and Inductive Melting.* Mater. Res. Soc. Symp. Proc., 1997. **465**: p. 371.

[b] The 6.19 wt% for total Rare Earth (REE2O3) oxides in SYNROC-C was the sum of the "x" wt.% of individual oxides which were not specified.

3.2. Melt Processing

Approximately 20g samples of feed stock were loosely placed into a covered alumina crucible. The samples were heated in air and in 1% H_2 (balance Argon) reducing atmosphere. Samples were heated at approximately 15°C/min, held at 1500°C for 20 minutes, and furnace cooled (powered off furnace). The resulting material was subsequently characterized.

3.2.1.Cr- Hollandite Multiphase Waste form

Figure 3-1 displays the microstructure and Table 3-3 tabulates the phases observed in Cr-Hollandite *with* Ti/TiO_2 buffer fabricated by Melt Processing 1500°C in 1%H_2/balance Argon atmosphere. It should be noted that this conditions comprising solid state reducing agents (Ti metal) as well as 1%H_2 gas environments represent the most extreme reducing studied in this work. In contrast to the single phase Cr-Hollandite which exhibited solid state sintering, the multiphase waste showed a microstructure indicative of melting. The targeted crystalline phases were formed including hollandite, zirconolite, perovskite/pyrochlore along with residual TiO_2.

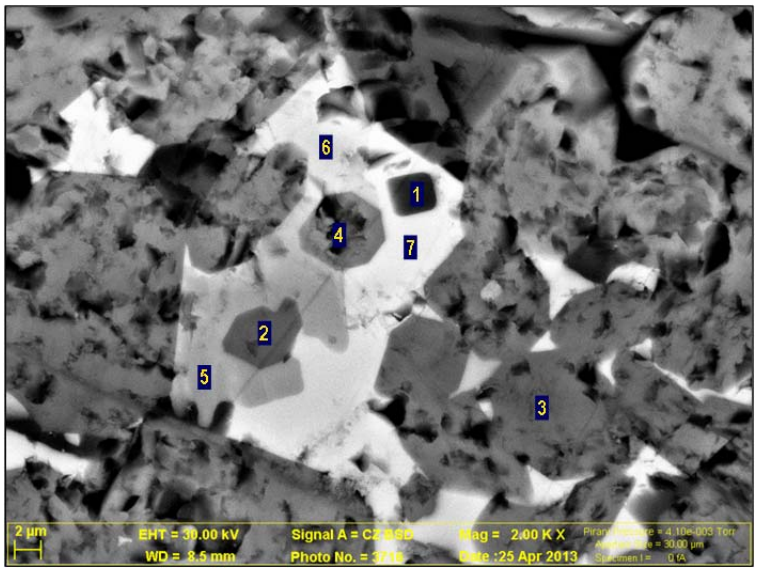

Figure 3-1. Cr-Hollandite Multiphase Waste Form (Cr-MPB1R-Ti) Fabricated Melt Processing 1500°C *with* Ti/TiO_2 buffer additions in 1%H_2/balance Argon atmosphere- Backscattered Electron Micrograph

Table 3-3. Cr-Hollandite Multiphase Waste Form (Cr-MPB1R-Ti) Fabricated Melt Processing 1500°C *with* Ti/TiO_2 buffer additions in 1%H_2/balance Argon atmosphere- Summary of Elements and Crystalline Phases *(*Crystalline phases determined from XRD measurements and EDAX elemental analysis)*

Spot	Elements (Major, Minor)	Crystalline Phases*
1	O,Ti, (Cr,Zr)	TiO_2
2,3,4	O,Ti,Cr,Ba, (Al,Ca,Zr,Cs,La,Nd)	Hollandite
5	O,Ti,Ca,Zr, (Y,Cr,Nd)	$CaZrTi_2O_7$
6	O,Ti, (Ca,Y,Zr,Ce,Nd)	$(A^{3+})_2TiO_5$
7	O,Ti, (Ca,Cr,La,Ce,Pr,Nd)	$(A^{3+})_2TiO_5$, $(La_{0.4}Ca_{0.4}TiO_3)$

3.2.2.Cr/Al/Fe Hollandite Multiphase Waste form

Figure 3-2 displays the microstructure and Table 3-4 tabulates the phases observed in Cr/Al/Fe-Hollandite *with* Ti/TiO_2 buffer fabricated by Melt Processing at 1500°C in $1\%H_2$/balance Argon atmosphere. The multiphase waste form showed grain structure indicative of melting. The targeted crystalline phases were formed including hollandite, zirconolite, perovskite/pyrochlore along with residual Al_2O_3, Fe_2O_3 and TiO_2.

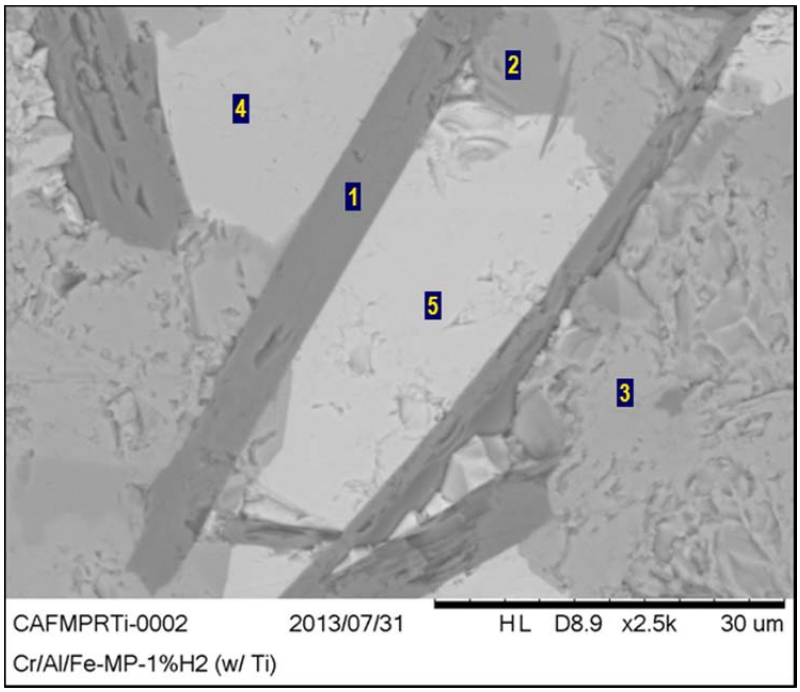

Figure 3-2. Cr/Al/Fe-Hollandite Fabricated Melt Processing at 1500°C *with* Ti/TiO_2 buffer additions in $1\%H_2$/balance Argon atmosphere Backscattered Electron Micrograph

Table 3-4. Cr/Al/Fe-Hollandite Fabricated by Melt Processing at 1500°C *with* Ti/TiO_2 buffer additions in $1\%H_2$/balance Argon atmosphere -Summary of Elements and Crystalline Phases *(*Crystalline phases determined from XRD measurements and EDAX elemental analysis)*

Spot	Elements (Major, Minor)	Crystalline Phases*
1	O,Al	Al_2O_3
2	O,Fe, (Ti,Al)	Fe_2O_3
3	O,Ti,Al,Cr,Ba, (Cs,Fe)	Hollandite
4	O,Ti,Zr,Al,Fe, (Cs,Ca,Ce,Nd)	$CaZrTi_2O_7$
5	O,Ti,Ca,Nd,Al, (Sc,Sr,Sm)	$(A^{+3}_xB^{+2}_{1-x})TiO_3$, $(A^{+3}_xB^{+2}_{1-x})_2Ti_2O_7$

3.3. Vacuum Induction Melting

Each composition was melted *with* and *without* a Ti/TiO_2 buffer in reducing conditions. Low oxygen levels resulting in reducing conditions were achieved by employing a vacuum induction melter operating at a pressure of 10^{-6} atm at 1500°C for 20 minutes.

3.3.1. Cr-Hollandite Multiphase Waste Form

Figure 3-3 displays the microstructure and Table 3-5 tabulates the phases observed in Cr -Hollandite *with* Ti/TiO_2 buffer fabricated by Vacuum Induction Melting at pressures ~ 10^{-6} atm. The oxygen partial pressure of ~ 10^{-6} atm during vacuum induction melting approximates the reducing conditions of an inert gas processing (pure Argon stream). The multiphase waste form showed a microstructure indicative of melting. The targeted crystalline phases were formed including hollandite, zirconolite, perovskite/pyrochlore along with residual TiO_2 was observed. Hollandite formed in needle-like microstructures and residual TiO_2 was found at the perovskite/titanate interface.

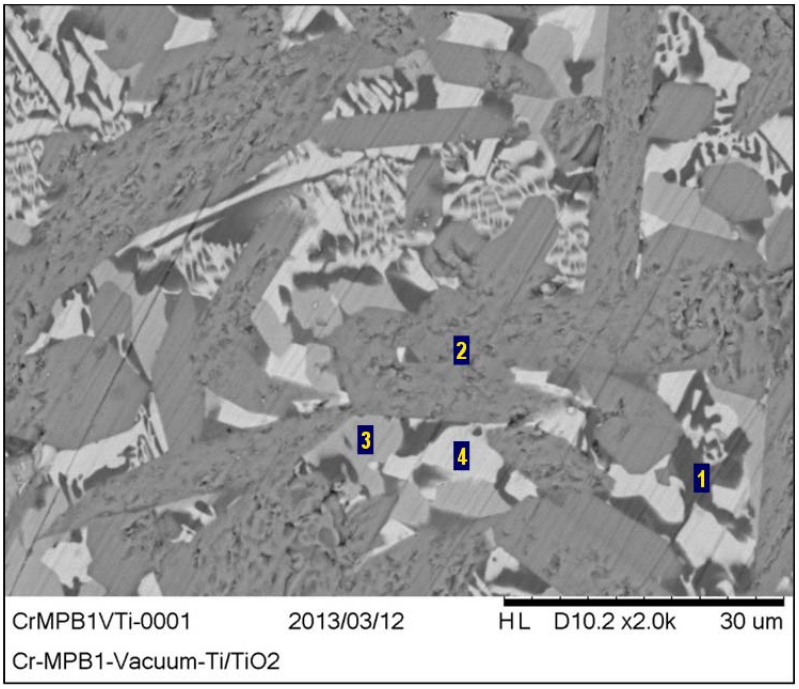

Figure 3-3. Cr-Hollandite Fabricated by Vacuum Induction Melting at 1500°C *with* Ti/TiO_2 buffer- Backscattered Electron Micrograph

Table 3-5. Cr-Hollandite Fabricated by Vacuum Induction Melting at 1500°C *with* Ti/TiO_2 buffer - Summary of Elements and Crystalline Phases *(*Crystalline phases determined from XRD measurements and EDAX elemental analysis)*

Spot	Elements (Major, Minor)	Crystalline Phases*
1	O,Ti, (Al,Cr,Zr,Ba,La,Ca,Cs)	TiO_2
2	O,Ti,Cr,Ba, (Al,Ca,Zr,Cs)	Hollandite
3	O,Ti,Zr, (Al,Ca,Cr,Y,La,Ce,Pr,Nd,Sm)	$CaZrTi_2O_7$
4	O,Ti,Nd, (Ca,Cr,Sr,Y,Ba,La,Ce,Pr,Sm)	$(Al^{3+})_2TiO_5$, $(La_{0.4}Ca_{0.4}TiO_3)$

3.3.2. Cr/Al/Fe Hollandite Multiphase Waste form

Figure 3-4 displays the microstructure and Table 3-6 tabulates the phases observed in Cr/Al/Fe - Hollandite *with* Ti/TiO_2 buffer fabricated by Vacuum Induction Melting at pressures ~ 10^{-6} atm. The multiphase waste form showed grain structure indicative of melting. The targeted crystalline phases were formed including hollandite, zirconolite, perovskite/pyrochlore along with residual Al_2O_3. In this sample,

the hollandite exhibited a needle-like microstructure and residual Al_2O_3 was found adjacent to the hollandite phase.

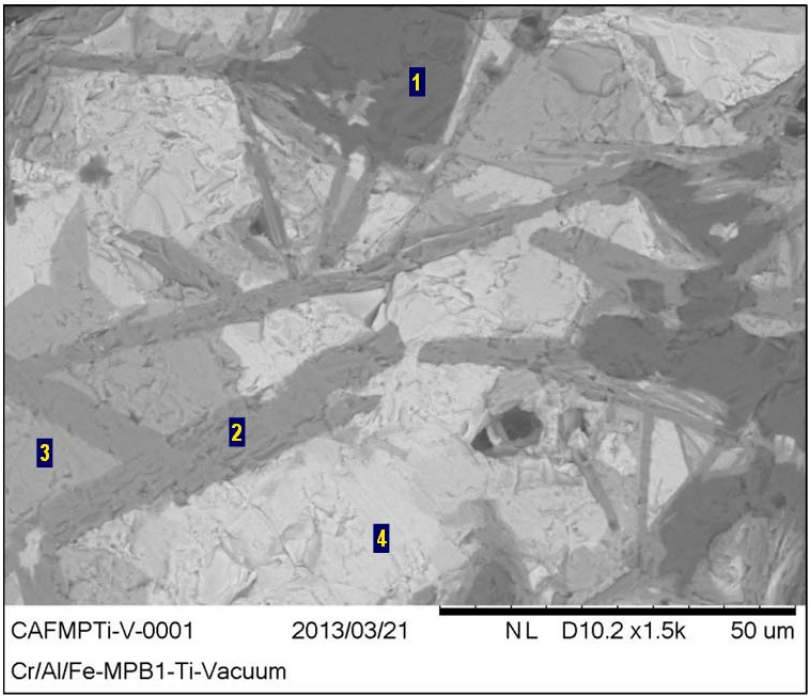

Figure 3-4. Cr/Al/Fe-Hollandite Fabricated by Vacuum Induction Melting at at 1500°C *with* Ti/TiO_2 buffer -Backscattered Electron Micrograph

Table 3-6. Cr/Al/Fe-Hollandite Fabricated by Vacuum Induction Melting at at 1500°C *with* Ti/TiO_2 buffer -Summary of Elements and Crystalline Phases *(*Crystalline phases determined from XRD measurements and EDAX elemental analysis)*

Spot	Elements (Major, Minor)	Crystalline Phases*
1	O,Al, (Ti,Cr)	Al_2O_3
2	O,Ti,Ba, (Al,Cr,Fe,Cs,Ce)	Hollandite, $BaTiO_3$
3	O,Ti,Zr, (Al,Ca,Fe,Y,Ce,Nd,Sm)	$CaZrTi_2O_7$
4	O,Al,Ti, (Cr,Fe,Sr,Ce,Nd)	$(A^{3+})_2TiO_5$

3.4. Spark Plasma Sintering (SPS)

Spark Plasma Sintering (SPS) was conducted on a Dr. Sinter Model SPS 515S from Metals Processing Inc. Approximately 1g of powder batch was mixed *with* a Ti/TiO_2 buffer and loaded in a graphite die for SPS processing at temperatures between 1080 and 1387°C.

3.4.1. Cr-Hollandite Multiphase Waste Form

Figure 3-5 displays the microstructure and Table 3-7 tabulates the phases observed in Cr -Hollandite *with* Ti/TiO_2 buffer fabricated by SPS at 1232°C. The multiphase waste form showed a fine grain structure (1-10 micron grain size) expected from rapid sintering techniques. The targeted crystalline phases were formed including hollandite, zirconolite, perovskite/pyrochlore along a Mo containing metallic alloy. The phases were observed in round microstructures typical of solid state sintering as opposed to needle-like crystalline materials observed in the melt processed samples.

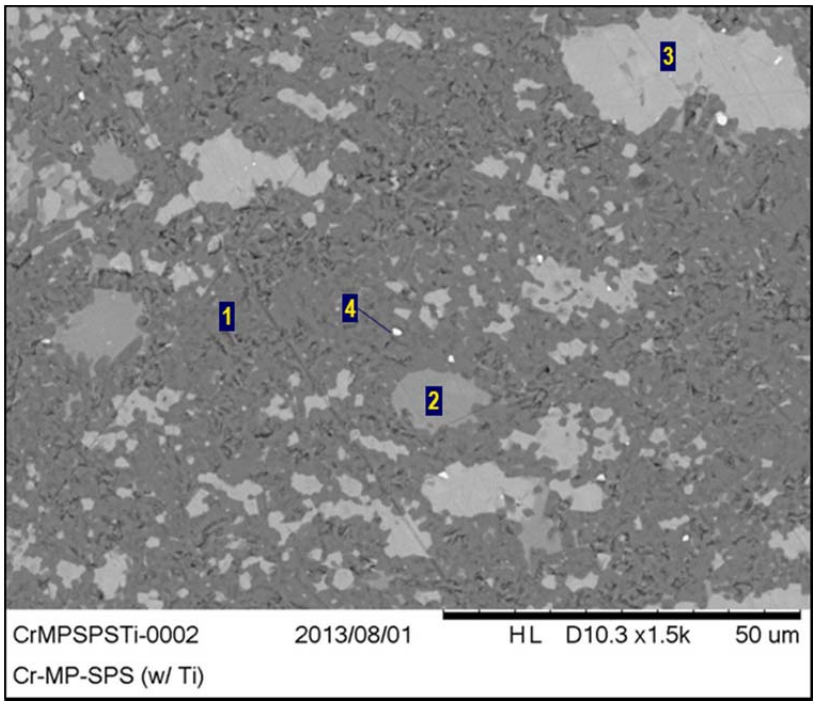

Figure 3-5. Cr -Hollandite Fabricated by SPS *with* Ti/TiO_2 buffer1232°C- Backscattered Electron Micrograph

Table 3-7. Cr-Hollandite Fabricated by SPS *with* Ti/TiO_2 buffer at 1232°C -Summary of Elements and Crystalline Phases *(*Crystalline phases determined from XRD measurements and EDAX elemental analysis)*

Spot	Elements (Major, Minor)	Crystalline Phases*
1	O,Ti,Ba,Fe,Cr,Al, (Cs,Zr)	Hollandite
2	O,Ti,Zr,Ca	$CaZrTi_2O_7$
3	O,Ti,Nd,Cr, (Zr,Sr,Y)	$(A^{+3}_xB^{+2}_{1-x})TiO_3$, $(A^{+3}_xB^{+2}_{1-x})_2Ti_2O_7$
4	Mo	Metallic

3.4.2. Cr/Al/Fe Hollandite Multiphase Waste form

Figure 3-6 displays the microstructure and Table 3-8 tabulates the phases observed in Cr/ Al/Fe -Hollandite *with* Ti/TiO_2 buffer fabricated by SPS at 1230°C. The multiphase waste form showed a similar microstructure compared to the Cr analogue. The targeted crystalline phases were formed including hollandite, zirconolite, perovskite/pyrochlore along a Mo containing metallic alloy.

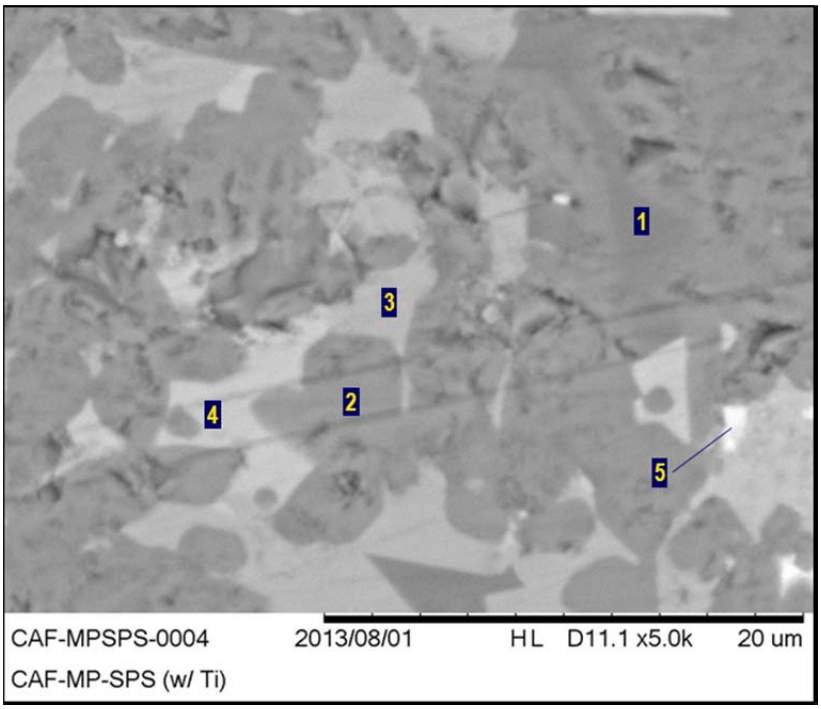

Figure 3-6. Cr/Al/Fe-Hollandite Fabricated by SPS *with* Ti/TiO_2 buffer at 1230°C Backscattered Electron Micrograph

Table 3-8. Cr/Al/Fe-Hollandite Fabricated by SPS *with* Ti/TiO_2 buffer at 1230°C-Summary of Elements and Crystalline Phases *(*Crystalline phases determined from XRD measurements and EDAX elemental analysis)*

Spot	Elements (Major, Minor)	Crystalline Phases*
1,2	O,Ti,Ba,Fe,Cr,Al, (Cs,Zr)	Hollandite
3	O,Ti,Zr,Ca, (Fe,Nd)	$(A^{+3}_xB^{+2}_{1-x})TiO_3$, $(A^{+3}_xB^{+2}_{1-x})_2Ti_2O_7$
4	O,Ti,Nd,Ca, (Sr,Y)	$CaZrTi_2O_7$
5	Te (Mo)	Metallic

3.5. Hot Pressing (HP)

The hot pressing procedure consisted of an initial 10°C/min ramp to a temperature of 1200°C where the sample was held for 2 hours followed by a decrease of the temperature to 1000°C in 15 minutes and finally shutting off the furnace and allowing the sample to cool to room temperature in approximately 2.5 hours. The pressure was maintained at 40+/-1 MPa with nitrogen gas supplied at a flow rate of 40 ml/min during the hot press procedure.

3.5.1. Cr-Hollandite Multiphase Waste Form

Figure 3-7 displays the microstructure and Table 3-9 tabulates the phases observed in Cr -Hollandite *with* Ti/TiO_2 buffer fabricated by HP at 1200°C. The multiphase waste form showed a fine grain structure as compared to the melt processed samples. The targeted crystalline phases were formed including hollandite, zirconolite, perovskite/pyrochlore along with residual TiO_2. Multiple titanates with distinct composition were observed.

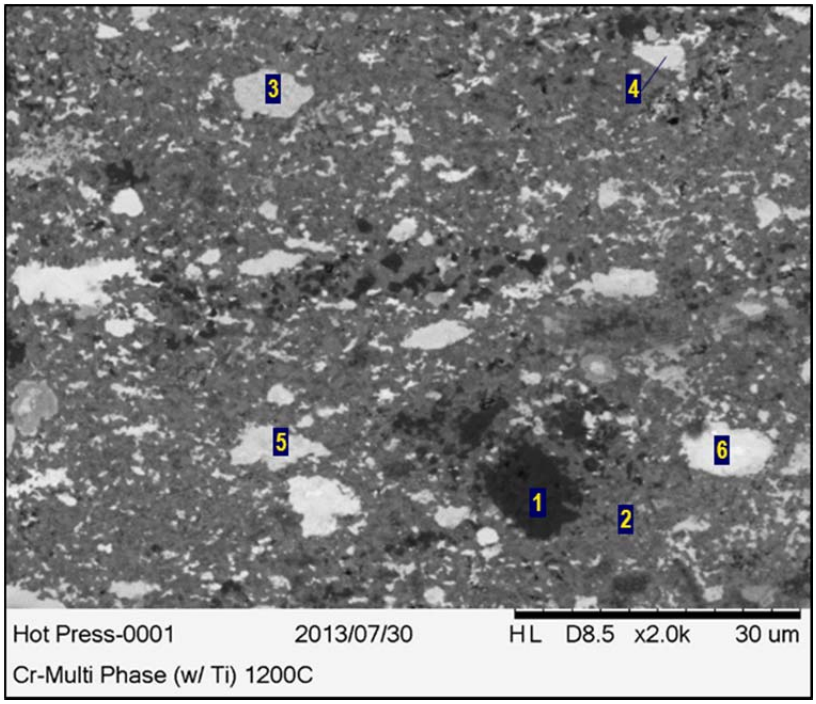

Figure 3-7. Cr-Hollandite Fabricated by HP 1200°C *with* Ti/TiO_2 buffer- Backscattered Electron Micrograph

Table 3-9. Cr-Hollandite Fabricated by HP 1200°C *with* Ti/TiO_2 buffer -Summary of Elements and Crystalline Phases *(*Crystalline phases determined from XRD measurements and EDAX elemental analysis)*

Spot	Elements (Major, Minor)	Crystalline Phases*
1	O,Ti	TiO_2
2		Hollandite
3	O,Ti,Zr, (Ca,Cr)	$CaZrTi_2O_7$
4	O,Ti,Ce	$(A^{+3}_xB^{+2}_{1-x})TiO_3$, $(A^{+3}_xB^{+2}_{1-x})_2Ti_2O_7$
5	O,Ti,La,Cr	$(A^{+3}_xB^{+2}_{1-x})TiO_3$, $(A^{+3}_xB^{+2}_{1-x})_2Ti_2O_7$
6	O,Ti,Nd,Pr, (Sr,Zr)	$(A^{+3}_xB^{+2}_{1-x})TiO_3$, $(A^{+3}_xB^{+2}_{1-x})_2Ti_2O_7$

3.5.2. Cr/Al/Fe Hollandite Multiphase Waste form

Figure 3-8 displays the microstructure and Table 3-10 tabulates the phases observed in Cr/Al/Fe -Hollandite *with* Ti/TiO_2 buffer fabricated by HP at 1200°C. The multiphase waste form a similar structure compared to the Cr analogue. A majority of the targeted crystalline phases were formed

including hollandite, perovskite/pyrochlore along with residual Al_2O_3 and TiO_2. Notably, the zirconolite phase was absent and multiple titanates with distinct composition were observed.

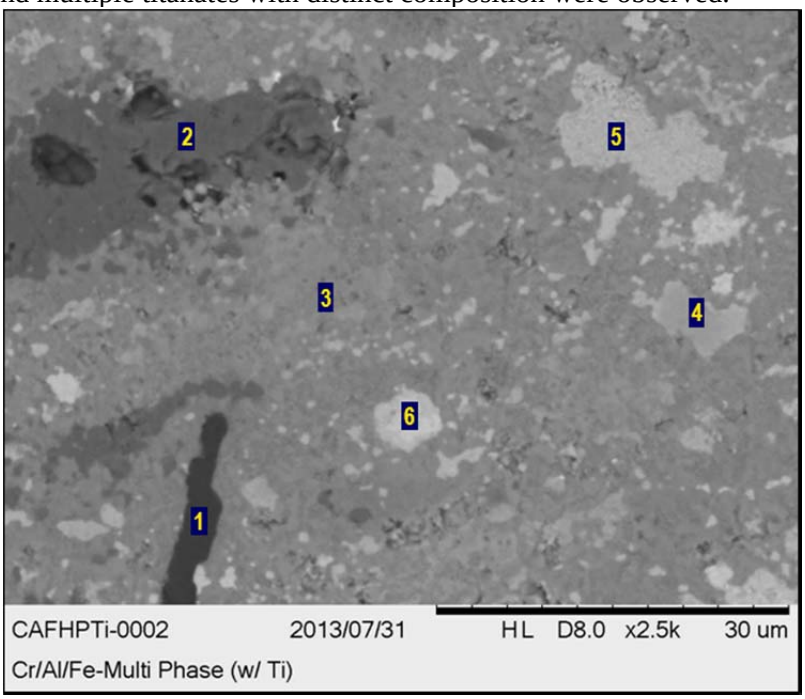

Figure 3-8. Cr/Al/Fe-Hollandite Fabricated by HP 1200°C *with* Ti/TiO_2 buffer Backscattered Electron Micrograph

Table 3-10. Cr/Al/Fe-Hollandite Fabricated by HP 1200°C *with* Ti/TiO_2 buffer -Summary of Elements and Crystalline Phases *(*Crystalline phases determined from XRD measurements and EDAX elemental analysis)*

Spot	Elements (Major, Minor)	Crystalline Phases*
1	O,Al	Al_2O_3
2	O,Ti	TiO_2
3	O,Ti,Ca,Ba,Fe,Cr, (Nd,Zr,Cs,Al)	Hollandite
4	O,Ti,Y, (Fe)	$(A^{+3})_2Ti_2O_7$
5	O,Ti,Ce,Nd,Ba	$(A^{+3}_xB^{+2}_{1-x})TiO_3$, $(A^{+3}_xB^{+2}_{1-x})_2Ti_2O_7$
6	O,Ti,Zr,Ca, (Fe,Nd)	$(A^{+3}_xB^{+2}_{1-x})TiO_3$, $(A^{+3}_xB^{+2}_{1-x})_2Ti_2O_7$

Table 3-11 presents a summary of the phase formation as a function of composition and processing conditions for multiphase waste forms fabricated in this study. In general, both compositions (Cr-MPB and Cr/Al/Fe-MPB) formed the major targeted phases under all processing conditions including Cs-containing hollandite. The pure Cr-analogue displayed some regions with incomplete melting and may need higher temperatures (1600°C) for melt processing. A metallic Mo containing alloy which was encapsulated in oxide phases was observed in SPS and HP samples using solid state sintering, while this phase was mostly absent in melt processed samples. An examination of crystallized ceramic material sampled from the crucible bottom as well as examination of the alumina crucible area in contact with the melt revealed Mo metal penetration into the alumina grain boundary regions of the crucible indicating the metal phases may have sank to the bottom during melt processing.

Table 3-11. Multiphase Characterization Summary[a]

Short Identifier[a]	Phases				Processing Conditions
	Cs-Hollandite $(Ba_xCs_y)(Ti,Al)^{+3}_{2x+y}(Ti^{+4}_{8-2x-y})O_{16}$	(4+) Zirconolite $CaZrTi_2O_7$	(2+/3+) Titanate (i.e. Pyroclore / Perovskite)[b] $(A^{2+})TiO_3$; $(A^{3+})_2Ti_2O_7$	Other	
Melt Processing					
Cr-MPB1A	X	X	X	TiO_2	Air
Cr-MPB1A-Ti	X	X	X	TiO_2	Air w/Ti-TiO_2
Cr-MPB1R	X	X	X		1% H_2
Cr-MPB1R-Ti	X	X	X	TiO_2	1% H_2 w/Ti-TiO_2
CAF-MPB1A	X	X	X		Air
CAF-MPB1A-Ti	X		X	TiO_2	Air w/Ti-TiO_2
CAF-MPB1R	X		X	$BaFe_{12}O_{19}$	1% H_2
CAF-MPB1R-Ti	X	X	X	$A^{+3}_2TiO_5$	1% H_2 w/Ti-TiO_2
Vacuum Induction Melting					
Cr-MPB1V	X		X		Vacuum
Cr-MPB1V-Ti	X	X	X		Vacuum w/Ti-TiO_2
CAF-MPB1V	X		X	Al_2O_3, $BaFe_{12}O_{19}$ $Ca_3Ti_8Al_{12}O_{37}$	Vacuum
CAF-MPB1V-Ti	X	X	X	Al_2O_3	Vacuum w/Ti-TiO_2
Spark Plasma Sintering (SPS)					
Cr-MP-SPS-1281	X	X	X		1281°C
Cr-MP-SPS-1387	X		X		1387°C
Cr-MP-SPS-Ti-1080	X	X	X	TiO_2, Cr_2O_3	1080°C w/Ti-TiO_2
Cr-MP-SPS-Ti-1232	X	X	X		1232°C w/Ti-TiO_2
CAF-MP-SPS-1230	X	X	X		1230°C
CAF-MP-SPS-1350	X	X	X		1350°C
CAF-MP-SPS-Ti-1200	X	X	X		1200°C w/Ti-TiO_2
CAF-MP-SPS-Ti-1230	X	X	X		1230°C w/Ti-TiO_2
Hot Pressing					
Cr-MP-HP	X	X	X	Cr_2O_3, ZrO_2	N_2, 1200°C
Cr-MP-HP-Ti	X	X	X	Cr_2O_3, ZrO_2	N_2, 1200°C, w/Ti-TiO_2
CAF-MP-HP	X	X	X		N_2, 1200°C
CAF-MP-HP-Ti	X	X	X	TiO_2	N_2, 1200°C, w/Ti-TiO_2

Melt processed samples exhibited larger grain sizes (~ 50-200 microns) with irregular, needle-like hollandite grains and large voids (> 10 microns). SPS and HP microstructures exhibited fine grain size (~

[a] "Cr-…" targeted $Ba_{1.0}Cs_{0.3}\mathbf{Cr}_{2.3}Ti_{5.7}O_{16}$ Hollandite; "CAF-…" targeted $Ba_{1.0}Cs_{0.3}\mathbf{Cr}_{1.0}\mathbf{Al}_{0.3}\mathbf{Fe}_{1.0}Ti_{5.7}O_{16}$ Hollandite.

[b] The A site in these titanate structures will accommodate a wide variety of species including alkaline and rare-earths. Additionally, the A site is substitutional in many compounds and will be mixed. More general formula include $(A^{+3}_xB^{+2}_{1-x})TiO_3$, $(A^{+3}_xB^{+2}_{1-x})_2Ti_2O_7$, etc. where A and B are tri- and di- valent species in the waste such as Ce, Nd, Pr, La, Ba, Y, Sr, etc.

10 micron) with smaller pores (~ 1micron) distributed throughout the microstructure. A detailed microstructural study of one composition (Cr/Al/Fe-Multiphase) *with* Ti/TiO_2 buffer across a wide variety of redox and processing conditions is presented in the following section.

4. DISCUSSION

There have been several comparative studies of crystalline ceramic waste forms produced by hot pressing and inductive melting.[7, 11] These prior studies have indicated that the specimens in general exhibited similar mineral compositions, with the exception of melted ceramics showing evidence of molybdate phases due to air processing with Mo containing waste streams. A major objective of this work was aimed at varying the composition and processing conditions in order to mitigate Cs-Mo molybdate phase formation. In addition, there was particular interest regarding differences in phase formation, elemental partitioning and microstructural variation as a function of waste form composition and processing conditions. In this study, common microstructural differences between samples processed by a melt and crystallization route and solid state sintering routes include an order of magnitude increase in grain size with melted ceramics along with an increase in porosity. Figure 4-1 displays the microstructure and Table 4-1 tabulates the phases observed Single Phase Hollandite *with* a Ti/TiO_2 buffer fabricated i) melt processing in air at 1500^{o}C, ii) melt processing in 1%H_2 balance Argon at 1500^{o}C, iii) HP at 1200^{o}C and iv) SPS at 1230^{o}C.

Firstly, significant Cs incorporation into the hollandite structure was observed via a melt processing route. The sample melt processed in air exhibited regions where incomplete melting occurred, most likely Cr rich regions which demonstrated this behavior in pure Cr-Hollandite analogues. The sample melt processed in hydrogen exhibited less of these incomplete melting regions. In addition to hollandite, a secondary Cs-phase $CsAlTiO_4$ was observed in samples melt processed in air and 1%H_2. Additional secondary phases associated with Fe-Ti were observed when melt processed under hydrogen gas. SPS and HP samples also showed evidence of secondary phases associated with Fe as well as metal inclusions. In general the single phase hollandite samples that were melt processed possessed both larger grain sizes and larger pores than the SPS and HP samples.

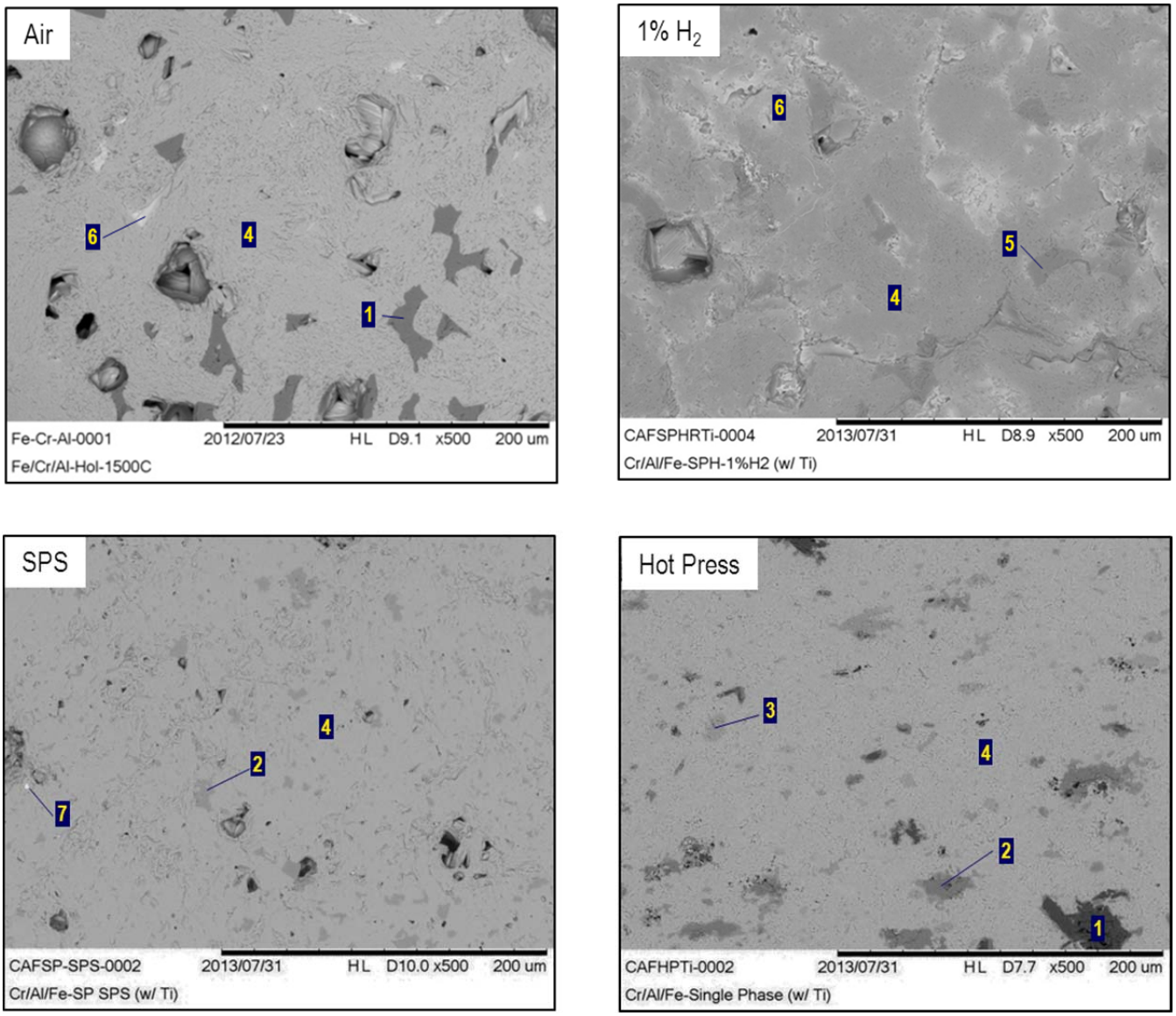

Figure 4-1. Single Phase Hollandite Cr/Al/Fe *with* Ti/TiO_2 Processing Comparison- Backscattered Electron Micrograph. (Air=Melting 1500°C in Air, 1%H_2=Melting 1500°C in 1%H_2 balance Argon gas, SPS=SPS at 1230°C, HP=HP at 1200°C at 40 MPa)

Table 4-1. Single Phase Hollandite Cr/Al/Fe *with* Ti/TiO_2 Processing Comparison -Summary of Elements and Crystalline Phases *(*Crystalline phases determined from XRD measurements and EDAX elemental analysis)*

Spot	Major Elements	Crystalline Phases*
1	O,Ti	TiO_2
2	O,Fe,Al	$FeAl_2O_4$
3	O,Fe	Fe_2O_3, FeO
4	O,Ti,Ba, (Cr,Al,Fe,Cs)	Hollandite
5	O,Ti,Fe	Titanate
6	O,Cs,Al, (Ti,Si)	$CsAlTiO_4$
7	Fe	Metallic

Figure 4-2 displays the microstructure and Table 4-2 tabulates the phases observed in Multiphase Waste Form Cr/Al/Fe Hollandite *with* a Ti/TiO_2 buffer fabricated i) melt processing in air at 1500°C, ii) melt processing in $1\%H_2$ balance Argon at 1500°C, iii) HP at 1200°C and iv) SPS at 1230°C. Several differences between samples were observed with regards to phase formation, grain size and microstructure and elemental partitioning. Similar to the observation in single phase systems, the sample melt processed in air was not completely melted (more refractory Cr rich regions). Due to the incomplete melting, metallic species were incorporated into the microstructure when processed in air, but were absent from the bulk microstructure when processed under hydrogen.

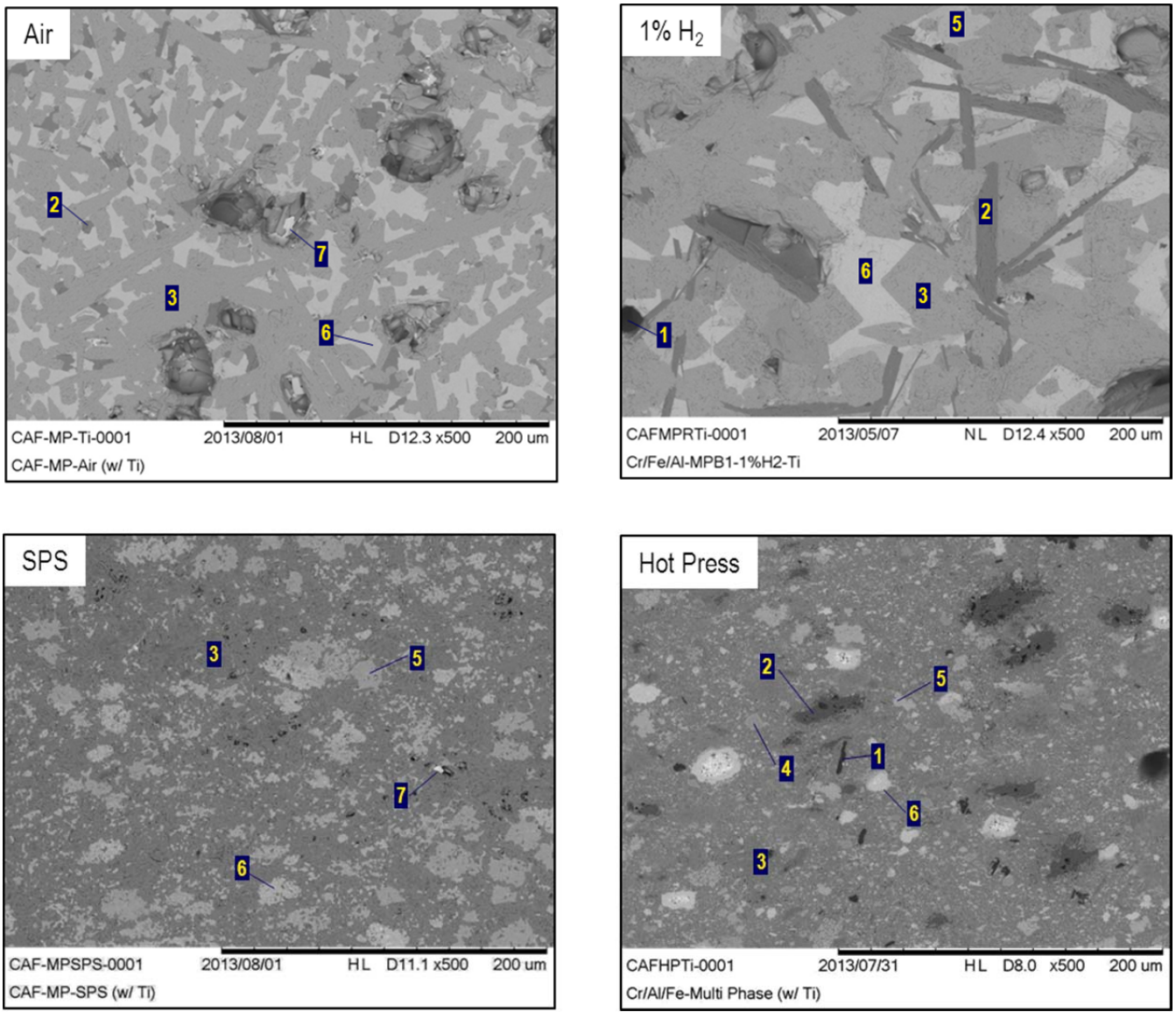

Figure 4-2. Multiphase Waste Form Cr/Al/Fe Hollandite *with* Ti/TiO_2 Processing Comparison-Backscattered Electron Micrograph

Table 4-2. Multiphase Waste Form Cr/Al/Fe Hollandite *with* Ti/TiO_2 Processing Comparison - Summary of Elements and Crystalline Phases *(*Crystalline phases determined from XRD measurements and EDAX elemental analysis)*

Spot	Elements (Major, Minor)	Crystalline Phases*
1	O,Al	Al_2O_3
2	O,Ti	TiO_2
3	O,Ti,Ca,Ba,Fe,Cr, (Nd,Zr,Cs,Al)	Hollandite
4	O,Ti,Y, (Fe)	$(A^{+3})_2Ti_2O_7$
5	O,Ti,Zr,Ca, (Fe,Nd)	$CaZrTi_2O_7$
6	O,Ti,Ce,Nd,Pr,La,Y, (Ba,Fe,Al,Cr)	$(A^{+3}_xB^{+2}_{1-x})TiO_3$, $(A^{+3}_xB^{+2}_{1-x})_2Ti_2O_7$
7	Mo	Metallic

Melting of the sample was enhanced when processed under reducing gas and a metallic alloy containing Mo was observed in the bottom of the alumina crucible. Enhanced melting resulted in larger grain size for the samples processed under hydrogen gas as compared to those melted in air. Samples melt processed in air exhibited the targeted phase with the exception of zirconolite. Samples melt processed in hydrogen exhibited the targeted phases of hollandite, perovskite/pyrochlore, zirconolite with residual TiO_2 and Al_2O_3.

The solid state sintering routes SPS and HP also demonstrated formation of the targeted phases. Hollandite, pervoskite/pyrochlore, zirconolite, metallic alloy and TiO_2 and Al_2O_3 were observed distributed in a network of fine grains with small residual pores. The titanate phases that incorporate M^{+3} rare earth elements were observed to be distinct titanate phases ($Nd_2Ti_2O_7$) with less degree of substitution as compared to the more homogeneous melt processed samples where a high degree of substitution and variation of composition within grains was observed. In general, our observations corroborate similar reports of melt processed versus solid state sintered waste forms in the literature showing that melt processed samples formed similar phases, however had larger grain sized along with large voids associated with the melt process; SPS and HP samples exhibited finer grain size with smaller voids. Metallic alloys were observed in the bulk of the sample for SPS and HP samples, but were found at the bottom of the crucible in melt processed trials.

5. RECOMMENDATIONS and PATH FORWARD

This work has demonstrated that waste streams of interest to the FCR&D program can be incorporated into crystalline ceramic waste forms by a melt and crystallization process. The targeted phases of hollandite, perovskite/pyrochlore, and zirconolite were similarly formed by a melt process as well as solid state sintering alternatives such as Hot Pressing and Spark Plasma Sintering. The principal differences between the synthesis procedures were the size of the voids (larger with melt process), grain size (order of magnitude larger for melt as compared to solid state processes), and ability to incorporate metallic alloys into the oxide matrix (Mo alloy sank to bottom of melt and crystallization process). The use of solid state buffer Ti/TiO_2 seems especially useful in promoting Cs incorporation into the hollandite phase and is recommended for use in subsequent melt processing trials. In fact, additives of Ti metal have been used to improve the electrical conductivity of powder batches in Cold Crucible Induction Melter trials and therefore serve a dual use. The two compositions studied in this report Cr and Cr/Al/Fe present a tradeoff between better phase formation- Cs incorporation into hollandite phase with less secondary phases

present (Cr) and the higher temperatures required to completely melt these more refractory compositions (estimated ~1600^{o}C).

Results presented in Figure 4-2 of multiphase waste forms based on Cr/Al/Fe-Hollandite indicate that these samples show similar phase formation when processed in air and 1%H_2 gas environments. The principal difference being the larger grain size due to enhanced melting in reducing gas environments. These results indicate that for a first melter trial, the targeted phases can be formed in air by utilizing Ti/TiO_2 additives which aid phase formation and improve the electrical conductivity. Ultimately, a melter run in reducing gas environments would be beneficial to study differences in phase formation and elemental partitioning. The electrical resistivity of SYNROC compositions has been previously measured to be on the order of 1 ohm*cm at temperatures near 1500^{o}C which was acceptable for CCIM processing demonstrations.[23] The electrical resistivity and viscosity of SRNL compositions of interest for FCR&D program should be studied as a function of temperature in preparation for a potential CCIM melter test in FY14.

6. REFERENCES

1. *Waste Forms Technology and Performance Final Report by National Research Council of the National Academies ISBN-10: 0-309-18733-8.* Waste Forms Technology and Performance Final Report by National Research Council of the National Academies ISBN-10: 0-309-18733-8, 2011.

2. Ringwood, A.E., et al., *IMMOBILIZATION OF HIGH-LEVEL NUCLEAR-REACTOR WASTES IN SYNROC.* Nature, 1979. 278(5701): p. 219-223.

3. Ringwood, A.E., et al., *SYNROC PROCESS - GEOCHEMICAL APPROACH TO NUCLEAR WASTE IMMOBILIZATION.* Geochemical Journal, 1979. 13(4): p. 141-165.

4. Perera, D.S., et al., *Application of Crystal Chemistry in the Development of Radioactive Wasteforms.* Advances in Technology of Materials and Materials Processing, 2004. 6(2): p. 214-217.

5. Stefanovsky, S.V., et al., *Inductive cold crucible melting of actinide-bearing murataite-based ceramics.* Journal of Alloys and Compounds, 2007. 444: p. 438-442.

6. Demine, A.V., et al., *High Level Waste Solidification Using a Cold Crucible Induction Melter.* Mater. Res. Soc. Symp. Proc., 2001. 663: p. 27-34.

7. Advocat, T., et al., *Alteration of Cold Crucible Melter Titanate-based Ceramics: Comparison with Hot-Pressed Titanate-based Ceramic.* Mater. Res. Soc. Symp. Proc., 1997. 465: p. 355-362

8. Leturcq, G., et al., *Solubility Study of Ti Zr-based Ceramics Designed to Immobilize Long-lived Radionuclides.* American Mineralogist, 2001. 86(7-8): p. 871-880.

9. Brinkman, K., et al., *Crystalline Ceramic Waste Forms: Reference Formulation Report* Report SRNL Technical Report SRNL-STI-2012-00281, FCRD-SWF-2012-000116, 2012.

10. Brinkman, K., et al., *Crystalline Ceramic Waste Forms: Report Detailing Data Collection in Support of Potential FY13 Pilot Scale Melter Test.* Report SRNL Technical Report FCRD-SWF-2012-000329, 2012.

11. Sobolev, I.A., et al., *Comparative Study of Synroc-C Ceramics Produced by Hot-Pressing and Inductive Melting.* Mater. Res. Soc. Symp. Proc., 1997. 465: p. 371.

12. Biagioni, C., P. Orlandi, and M. Pasero, *Ankangite from the Monte Arsiccio mine (Apuan Alps, Tuscany, Italy): occurrence, crystal structure, and classification problems in cryptomelane group minerals.* Periodico Di Mineralogia, 2009. 78(2): p. 3-11.

13. Carter, M.L., E.R. Vance, and H. Li, *Hollandite-rich ceramic melts for the immobolisation of Cs.* Mater. Res. Soc. Symp. Proc., 2003. 807: p. 249.

14. Aubin-Chevaldonnet, V., et al., *Preparation and Characterization of* $(Ba,Cs)(M,Ti)_8O_{16}$ *(M =* Al^{3+}, Fe^{3+}, Ga^{3+}, Cr^{3+}, Sc^{3+}, Mg^{2+}*) Hollandite Ceramics Developed for Radioactive Cesium Immmobilization.* Journal of Nuclear Materials, 2007. 366(1-2): p. 137-160.

15. Carter, M.L., E.R. Vance, and H. Li, *Hollandite-rice Ceramic Melts for Immobilization of Cs.* Mat. Res. Soc. Symp. Proc., 2004.

16. Carter, M.L., et al., *Mn Oxidation States in $Ba_xCs_yMn_zTi_{8-z}O_{16}$.* Mat. Res. Soc. Symp. Proc., 2004.

17. Whittle, K.R., et al., *Structural Studies of Hollandite-Based Radioactive Waste Forms.* Mat. Res. Soc. Symp. Proc., 2004. 807.

18. Buykx, W.J., et al., *TITANATE CERAMICS FOR THE IMMOBILIZATION OF SODIUM-BEARING HIGH-LEVEL NUCLEAR WASTE.* Journal of the American Ceramic Society, 1988. 71(8): p. 678-688.

19. Potdar, H.S., et al., *A simple chemical co-precipitation/calcination route for the synthesis of simulated synroc-B and synroc-C powders.* Materials Chemistry and Physics, 2010. 123(2-3): p. 695-699.

20. Amoroso, J., et al., *Single Phase Melt Processed Hollandite Waste Forms for Nuclear Waste Immobilization.* Journal of Alloys and Compounds, 2013. submitted.

21. Billings, A.L., et al., *Preliminary Study of Ceramics for Immobilization of Advanced Fuel Cycle Reprocessing Wastes.* U.S. Department of Energy Report: FCRD-WAST-2010-000158, SRNL-STI-2010-00560, 2010. Savannah River National Laboratory, Aiken, SC.

22. Brinkman, K., K.M. Fox, and M. Tang, *Development of Crystalline Ceramics for Immobilization of Advanced Fuel Cycle Reprocessing Wastes.* U.S. Department of Energy Report: FCRD-SWF-2011-000310, SRNL-STI-2011-00516, 2011. Savannah River National Laboratory, Aiken, SC.

23. Knyazev, O.A., S.V. Stefanovskii, and D.B. Lopukh, *Determination of Melt Electric Resistivity at IMCC.* Waste Management Conference, February 25-March 1, 2001 Tucson AZ, 2001.